

Surface Texture of Deformable Robotic Fingertips for a Stable Grasp under both Dry and Wet Conditions

Kaori Mizushima¹, Toshihiro Nishimura¹, *Student Member, IEEE*, Yosuke Suzuki², *Member, IEEE*
Tokuo Tsuji², *Member, IEEE*, and Tetsuyou Watanabe², *Member, IEEE*

Abstract— This study investigates the effect of the surface texture of soft deformable fingertips on the maximum resistible force under dry and wet conditions, and proposes a new hybrid structure that provides a stable grasp under both conditions. One definition of stable grasp is the capability of balancing a large external force or moment while grasping. For soft fingertips, both the friction and surface deformation contribute to the stability. Therefore, we investigate the maximum resistible force, which is defined as the maximum tangential force at which the fingertip can maintain contact when applying and increasing the tangential/shear force. We investigate the slit textures with primitive patterns and demonstrate that the non-pattern performs the best under dry conditions, whereas the horizontal slit pattern performs the best under wet (oily) conditions. Based on this, a concentric hybrid texture of the two patterns is proposed, and its effectiveness is verified by a grasping test.

Index Terms— End effectors, Friction, Grasping, Lubrication, Rough surfaces, Surface texture

I. INTRODUCTION

ROBOTS are entering the human environment and the demand for them to substitute manual daily work is increasing. The robotic hand is the key tool to conduct the work, and there are numerous requirements. One important requirement that has not yet been extensively explored is the grasping under wet conditions. Note that in this paper, wet is defined as “wet with water, oil, or other types of liquids.” Water, oil, and other liquids are media that are used daily, and thus the grasping of objects under wet conditions is common in daily life. However, conventional robotic hands implicitly assume application under dry conditions, with the exception of a few studies [1]–[3]. This study challenges the stable grasping of

objects irrespective of surface conditions, focusing on the surface structure of robotic fingertips.

A. Soft surface

Robotic hands with soft surfaces are becoming more attractive [2], [4]–[8]. Fluids are easily adaptable to external environments, thus, they have thus been utilized to compose fingertips. In particular, pneumatic systems are often used [9]–[19]. Liquids are also candidate materials for soft fingers [20]–[24]. The soft surface provides a low contact impact, safe interaction between the object and environment, high friction, and adaptation to the object shape. These benefits are attributed to the surface deformation, which is also critical to developing a fingertip surface structure to cope with both dry and wet conditions. The surface deformation can change the surface structure and then facilitate the embedding of multiple functions on the surface. In particular, the deformation is higher in fluid fingertips composed of liquids [20]–[23] than those composed of the other materials such as air or silicone rubber. With this in mind, this study focused on soft/fluid robotic fingertips.

One definition of stable grasp is the capability of balancing large external forces or moments during grasping. In soft fingertips, both friction and surface deformation contribute to the stability. Therefore, we define the maximum resistible force as the maximum tangential force at which the fingertip can maintain contact when applying and increasing the tangential/shear force [25], [26]. Friction on soft surfaces and the effects of surface deformation have been investigated by Kao et al. [27]–[31], Hirai et al. [32] [33], Ciocarlie et al. [34], and Watanabe et al. [25], [26], [35]. However, these investigations were conducted for dry conditions. Kitchen robots are an example of coping with wet conditions [1], [36]–[39], as are robotic hands for underwater manipulation [2] [3]. The IRT Research Initiative developed a kitchen robot that could wash dishes [1], where a thick glove prevented the robotic hand from becoming wet. Other kitchen robots utilized kitchen tools and avoided the necessity of dealing directly with wet conditions. However, grasping oily foodstuffs or dishes and stowing wet cups are common in daily life, and grasping objects under wet conditions is worthy of investigation. Robotic hands that function underwater have been developed [2] [3], but the grasping forces were provided by fluid pressure

Manuscript received: February, 15, 2017; Revised May, 10, 2017; Accepted June, 1, 2017.

This paper was recommended for publication by Editor Han Ding upon evaluation of the Associate Editor and Reviewers' comments. This work was partly supported by JSPS KAKENHI Grant Number 16H04298.

¹K. Mizushima and T. Nishimura are with the Graduated school of Natural science and Technology, Kanazawa University, Kakuma-machi, Kanazawa, 9201192 Japan (e-mail: k_mizushima@stu.kanazawa-u.ac.jp).

²Y. Suzuki, T. Tsuji, and T. Watanabe are with the Faculty of Mechanical Engineering, Institute of Science and Engineering, Kanazawa University, Kakuma-machi, Kanazawa, 9201192 Japan (e-mail: te-watanabe@ieee.org).

Digital Object Identifier (DOI): see top of this page.

control, and the effects of friction and the deformation during grasping were not investigated.

B. Surface structure to avoid slippage

Some robots have a special surface to avoid slippage. Dadkhah et al. developed a gripper using an electrostatic and gecko-like adhesive [40]. Hawkes et al. developed a thin film resembling the leg surface of a gecko [41] and utilized the film to construct a gripper. However, wet conditions were not considered.

Friction under wet conditions has been investigated in the tribology field. Tsipenyuk et al. [42] and Varenberg et al. [43] showed that the hexagonal surface increases drainage performance and improves friction on surfaces under oily conditions. Drotlef et al. [44] developed a material with an uneven surface resembling a frog leg to increase friction under wet conditions. It is well-known that commonly-used shoe soles and car tires have grooves to drain rainwater and increase friction under wet conditions [45], [46]. As pointed out in [47], [48], even in the tribology field, no research has been conducted providing a design criterion for surface patterns/textures, and the individual design issue must be based on empirical knowledge. Thus, in this study, we experimentally investigate the surface patterns to produce a stable grasp under both wet and dry conditions.

C. Contribution

This study aims to develop a novel surface texture for the deformable fluid fingertip [20]–[23] (Fig. 1), which provides high resistible forces under both dry and wet conditions. The main contributions of this study are as follows:

- We investigated the effect of the surface textures on the resistible force and showed which textures provide a large resistible force under dry and wet conditions.
- Based on the investigation, a novel surface texture that provides large resistible forces under both dry and wet conditions is presented.

The rest of this paper is organized as follows. The subsequent section presents the results of the preliminary experiments. Based on these results, the investigations of the slit texture patterns are then described. Based on the investigation, hybrid texture patterns are proposed and evaluated. Lastly, the summary is presented.

II. BASIC STRUCTURE OF FINGERTIP

A. Fluid fingertip

In this study, the fluid fingertip illustrated in Fig. 2 was utilized, and a surface texture was embedded and examined. The fingertip base is a rounded square with a width of 45 mm, with two holes connected to a pump and pressure sensor (Keyence AP-12S). A nitrile rubber film covers the base and was filled with a compressive fluid, chain saw oil (ISO VG100). The pressure sensor senses the fluid pressure, which is controlled by the pump.

B. Surface texture

A silicone texture was coated on the rubber film. The coated

area was 35 mm × 35 mm and the texture was provided by a silicone sealant (Hapio seal pro, Kanpe Hapio), which deforms according to the expansion and contraction of the rubber film. The mold for the texture pattern was built by a 3D printer (Stratasys uPrintSE). After placing the mold on the rubber film, the silicone sealant was applied. This was the fabrication process.

III. INVESTIGATION OF PRIMITIVE TEXTURE PATTERNS

We investigated the effect of primitive texture patterns on the maximum resistible force. Fig. 3 displays the investigated texture patterns. The following primitive patterns were selected: non-pattern, vertical and horizontal grooves, and dot-pattern. Here, the terms “vertical” and “horizontal” refer to the patterns constructed by lines parallel and perpendicular to the loading direction, respectively. The interval distance between grooves or dots was set to 1 mm to correspond to the resolution of the 3D printer. The target object grasped was a silicon cube with an edge of 35 mm, mass of 30.4 g, and hardness of 50 (Shore A). The flat surface was selected because it is suitable for maintaining a uniform wet condition in the grasp area and for the investigation of resistible force.



Fig. 1. Fluid fingertip with surface texture

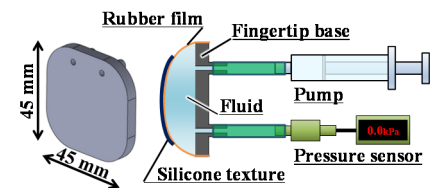


Fig. 2. Basic structure of the fluid fingertip

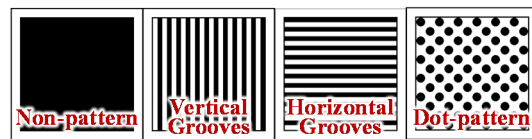


Fig. 3. Surface texture patterns for the investigation

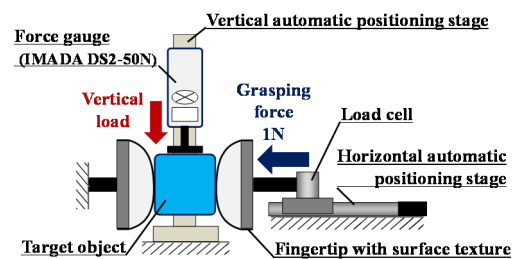


Fig. 4. Schematic view of experimental setup for resistible force test

A. Experimental setup and method

Fig. 4 shows the experimental setup when utilizing the fluid fingertips. The resistible force was investigated by applying a vertical load while grasping the target object. One fingertip was fixed by the vise, while the other was fixed to the handmade parallel-beam structure-based load cell [21] (allowable load: 10 N; resolution: 0.01 N) attached to the horizontal automatic positioning stage (Oriental motor ELSM2XF030K). The force gauge (IMADA DS2-50N) was fixed to the vertical automatic positioning stage (IMADA MX2-500N) that moves in the vertical direction to apply a load on the grasped target object.

First, the object was placed on a stage between the fingertips, and the horizontal automatic positioning stage was controlled such that the object was grasped with a grasping force of 1 N. The stage under the object was removed after grasping. The vertical automatic positioning stage for loading was controlled such that the force gauge could contact the grasped object with a load of 0 N. This was the initial state. From the initial state, the vertical load was increased by moving the vertical stage slowly (at 50 mm/min) until the object dropped. The maximum value of the load is referred to as the maximum resistible force in the given experimental condition. The experiment was carried out four times for each texture pattern. Dry and oily conditions were examined. Water was not utilized, because its viscosity is too low to maintain uniform and constant conditions. It should be noted that from elastohydrodynamic lubrication (EHL) theory (see Appendix), the oily condition (thickness of the oil film) can be kept constant if the supplying oil is sufficient and the grasping force is constant. To produce the dry condition, we cleaned the surface with ethanol and waited until the ethanol volatilized. Namely, the dry and oily conditions were kept constant through all investigations.

B. Rigid and flat plate fingertip

To observe the effect of the texture patterns only on friction, we conducted a preliminary experiment where rigid and flat plates were utilized for the fingertips instead of the fluid fingertips shown in Fig. 4. Because there is no surface deformation, the resistible force is identical to the frictional force.

Fig. 5 displays the results. Under the dry condition, the non-pattern provided the largest maximum resistible force, while the other patterns provided smaller forces. In contrast, under the oily condition, the non-pattern provided the smallest maximum resistible force. It is observed that the oily condition decreased the friction and the texture patterns reduced this decrease.

Fig. 6 shows the relationship between the apparent contact area and maximum resistible force. The apparent area is a convex area of 30 mm × 30 mm, which is depicted by the red area in Fig. 7. The maximum resistible force is observed to increase with the apparent contact area. We considered that the oily condition provides a fluid film at the contact area, decreasing the friction, but the texture could reduce the friction decrease because of the grooves. The grooves could reduce the thickness of the fluid film at the convex area of the texture. The decrease in fluid film thickness corresponds to the increase in friction from Newton's law of viscosity.

C. Fluid fingertip

The surface of a fluid fingertip can deform. It is thus expected that the deformation can increase the contact area and resistible force. The deformation can also increase or decrease the grooves on the textures, the effect on the resistible force of which is unclear. This was investigated in this study. The experiment was conducted using fluid fingertips with the same texture patterns at the surface. The fluid pressure was 4 kPa. The results are presented in Fig. 8.

Under the dry condition, we obtained the same tendency as the previous experimental results; the maximum resistible force increased with the apparent contact area. However, the difference in maximum resistible force between the non-pattern and the other patterns was large. The horizontal-grooves and dot patterns have cavities/hollows or breaks in the loading direction. A local large bending deformation occurs because of the small second moment of area, and the resistible force thus decreases [25], [26]. Therefore, the resistible forces for the two patterns were small.

Under the oily condition, the fingertips with the non-pattern failed to grasp, while the fingertips with the other patterns succeeded, although the maximum resistible force was small. Slippage was prevented by the textures.

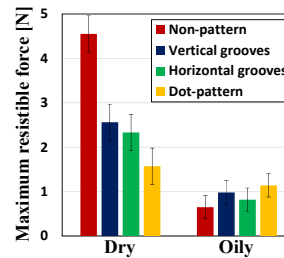


Fig. 5. Maximum resistible force when grasping a silicone cube by the rigid and flat plates under dry and oily conditions

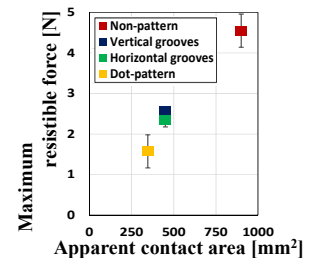


Fig. 6. Relationship between the apparent contact area and maximum resistible force when grasping a silicone cube by the rigid and flat plates under dry conditions

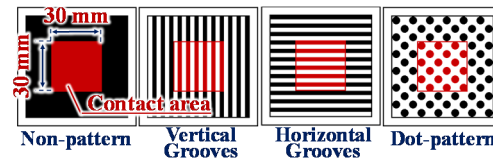


Fig. 7. Schematic view of the apparent contact area for each texture pattern

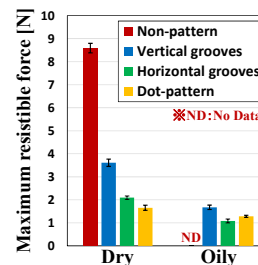


Fig. 8. Maximum resistible force when grasping a silicone cube by the fluid fingertips under dry and oily conditions

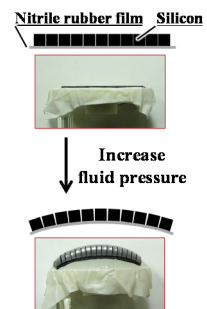


Fig. 9. Arrangement change by increasing fluid pressure

IV. INVESTIGATION OF SLIT TEXTURE

The preliminary experiments suggested that

- Under the dry condition, the maximum resistible force increased with the apparent contact area.
- Under the oily condition, the drainage effect of the surface texture pattern is useful for grasping.
- The increases in both apparent contact area and drainage ability are preferable for stable grasping under both conditions.

To achieve a stable grasp regardless of the condition, a texture pattern that provides a large apparent contact area and reduces the oil lubrication effects on the resistible force is preferable. Here, we focus on the deformation of the fluid fingertip. The elastic film deforms by the change in fluid pressure or external load. This deformation can change the roughness. Based on this, a slit texture pattern was selected (see Fig. 9). The increase in fluid pressure expands the slit and the groove texture is obtained, as shown in Fig. 9. The apparent contact area is larger than the textures with grooves (Fig. 3). A slit pattern was fabricated by cutting the silicone sealant, after coating the rubber film with the silicone sealant. The primitive slit texture patterns displayed in Fig. 10 were selected and investigated for easy fabrication and to understand the effects of different slit directions.

It is noted that the fluid fingertip provides uniform contact pressure, and the pressure is very low. Thus, an increase in the grasping force is less effective at increasing the ratio of actual to apparent contact area (actual contact area is proportional to frictional force) than increasing just the apparent contact area. If the grasping force is changed, the obtained values of the maximum resistible force will be different, whereas the relative trend in the differences between the different conditions will be similar. We thus conducted the investigations while fixing the grasping force value to 1 N.

A. Effects of fluid pressure and slit pattern

The fluid pressure of the fluid fingertips affects the stiffness and deformability, and thus the arrangement or pitch of the texture pattern. If the fluid pressure is low and, therefore, fingertip stiffness, surface extension, or bulge are small, the slit expansion will be small and the apparent contact area will be large. Then, a large resistible force is expected under the dry condition; however, a small resistible force is expected under the oily condition. If the fluid pressure is high, antipodal results are expected. Therefore, we investigated the effects of the fluid pressure as well as the slit patterns. In order to preserve the deformability function of the fluid fingertip, a low thickness of the silicone sealant is required. Thus, the range of changeable thicknesses is narrow, and the thickness was set to (constant) 1 mm. If the depth of the slits is shorter than the thickness, the deformability of the fluid fingertip cannot be utilized and the drainage effect can be too low. Thus, the depth was set to the same value as the thickness. The interval between the slits was set to 2 mm. The available range of fluid pressure was 2–8 kPa. Fluid pressures of 2, 4, 6, and 8 kPa were then investigated.

Fig. 11 presents the results. First, the results with a fluid pressure of 4 kPa were compared with the results shown in Fig. 8. The non-pattern exhibited a similar performance. The remaining slit patterns had larger resistible forces than the groove patterns under both conditions. These results indicate that the slit textures exhibit the drainage ability.

The comparison of the patterns under dry conditions indicates that the non-pattern texture provided the largest maximum resistible forces, followed by the vertical slit texture. There is no break in the loading direction in these patterns, providing large contact areas. In contrast, there are breaks in the

loading direction in the horizontal and grid slit patterns. The load increased the deformation of the texture pattern and the breaks in the loading direction, and decreased the contact area, which corresponds to a decrease in resistible force. Fig. 12 (a) shows the schematic view of the hypothesis of the phenomenon where the contact area was limited to that around the corners of the breaks.

Under oily conditions, the grasp failed with the non-pattern texture, and the drainage effect of the slit texture patterns was confirmed. For a fluid pressure of 2 kPa, the horizontal slits provided an extremely high maximum resistible force. The grid texture also provided a large maximum resistible force. It is considered that no break resulted from oil lubrication (which indicates a large R in (1) of the Appendix: EHL theory), and the resistible force decreased. The breaks were effective at reducing the lubrication (which indicates small R in (1)), particularly the breaks in the loading direction. As shown in Fig. 12 (b), it is considered that the corners of the breaks reduce the oil layer and the contact area is similar to that under the dry condition.

The lowest fluid pressure (2 kPa) performed the best under both conditions. At low fluid pressures, the deformation is large and large contact areas were obtained. The large slit expansion due to the high fluid pressure indicates a large R in (1), which corresponds to a low friction. These are considered the reasons for the best performance at the lowest fluid pressure.



Fig. 10. Slit texture patterns

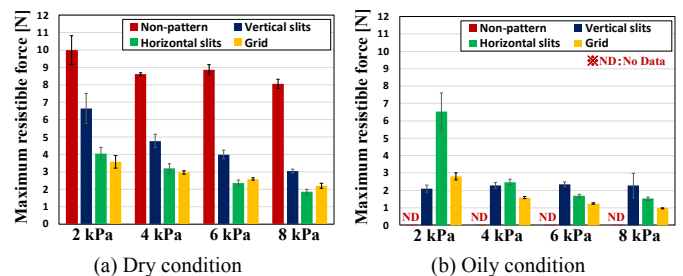


Fig. 11. Maximum resistible force for various fluid pressures and various slit texture patterns

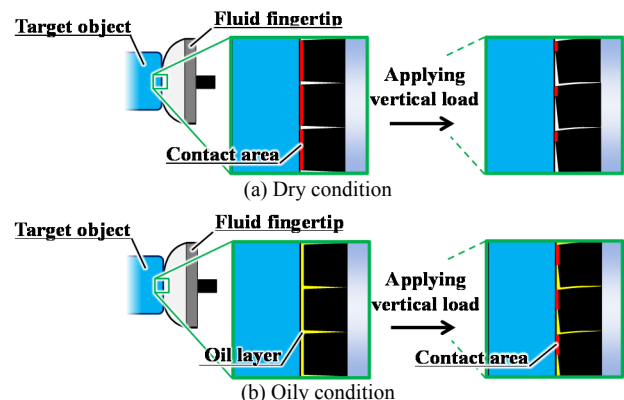


Fig. 12. Hypothesis of local surface deformation for the horizontal and grid slit texture patterns

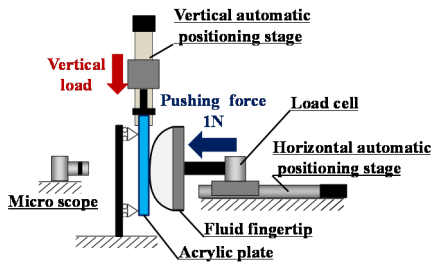


Fig. 13. Schematic view of the experimental setup for observing the contact area

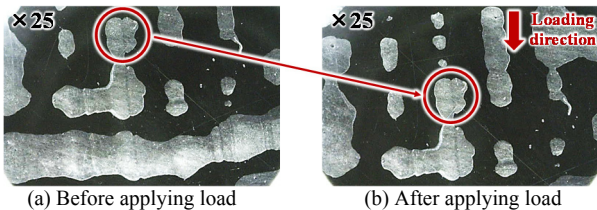


Fig. 14. Contact area of the non-pattern before and after applying a load under the dry condition

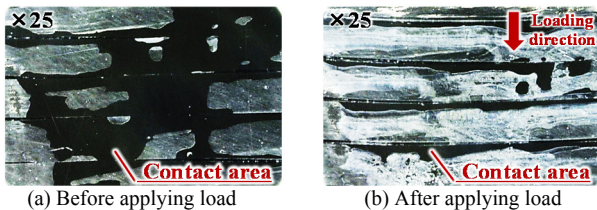


Fig. 15. Contact area of the horizontal slits before and after applying a load under the dry condition

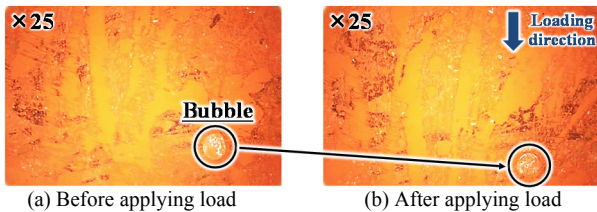


Fig. 16. Contact area of the non-pattern before and after applying a load under the oily condition; the oil is colored in red

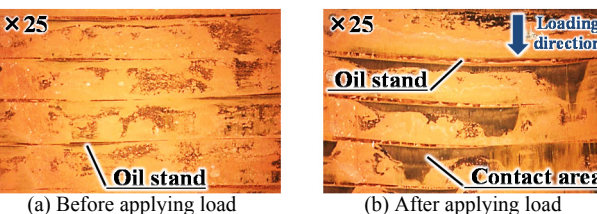


Fig. 17. Contact area of the horizontal slits before and after applying a load under the oily condition; the oil is colored in red.

B. Observation of contact area

To confirm the hypothesis shown in Fig. 12, the contact area was observed. Fig. 13 shows the experimental setup. The fingertip with the non-pattern and horizontal slit texture patterns was pressed against a transparent acrylic plate with a load of 1 N and fluid pressure of 2 kPa. The load was controlled by the same system as that shown in Fig. 4. The contact area was observed by a microscope (Keyence VHX-2000). We investigated dry and oily conditions.

Figs. 14 and 15 present the results under the dry condition where the black area corresponds to the contact area. With the non-pattern (Fig. 14), the component of the contact area hardly

changed with the loading. In contrast, at the horizontal slits (Fig. 15), the upper edge area of each segment maintained contact only after applying the load, which confirms the hypothesis shown in Fig. 12 (a). Figs. 16 and 17 present the results under the oily condition, where the black area corresponds to the contact area. With the non-pattern (Fig. 16), the contact area was covered by the oil film, and no clear contact area was observed when loading. With the horizontal slits (Fig. 17), oil stands (brown colored area) was observed at the breaks/slits, and the contact area around the upper edge of each segment between the slits expanded downwards with the increase in loading. These results confirm the hypothesis shown in Fig. 12 (b).

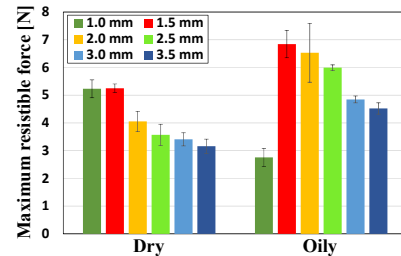


Fig. 18. Maximum resistible force for various slit intervals; the horizontal slit texture pattern with a fluid pressure of 2 kPa was evaluated under dry and oily conditions

C. Effect of slit interval

The effect of the slit interval was evaluated using the fingertip with the horizontal slit texture pattern and a fluid pressure of 2 kPa, which was the most effective for drainage, as shown in Fig. 11 (b). The range of evaluated intervals was 1.0–3.5 mm. The remaining experimental conditions were as described in section IV.A. Fig. 18 shows these results. The maximum resistible force increased with the decrease in interval under both conditions. As described in the previous subsection, under the dry condition, the main contact area is the upper edge area of each segment and the increase in contact area increases the friction when the contact pressure is low. If applying EHL theory (see Appendix) to the cases for the oily condition, the interval corresponds to the equivalent contact radius R , and the other parameters are regarded as constant. A small R produces a thin fluid film, which leads to a large friction. It should be noted that if the interval is too small, the slit segment will not be able to resist the tangential shear force/stress, because of the low rigidity/stiffness in the bending, thus, it flexes and the friction decreases [25], [26]. Therefore, the performance at the interval of 1.0 mm was lower than expected, especially under the oily condition. The other interesting point is that the maximum resistible force under the oily condition is larger than that for the dry condition, except for the interval of 1.0 mm. In summary, the interval of 1.5 mm performed the best in the range investigated. The interval should be minimized within the range that the segment can maintain its structure and not flex.

V. HYBRID SLIT TEXTURE PATTERN

To summarize the aforementioned investigations,

- Under the dry condition, the non-pattern performed the best.

- Under the oily condition, the horizontal slits performed the best, and the maximum resistible force was larger than that under the dry condition.

The slit interval of 1.5 mm and fluid pressure of 2 kPa performed the best.

The maximum resistible force for the horizontal slits under the dry condition was approximately 40% of that for the non-pattern, which is too small. Therefore, we considered a hybrid texture pattern of the non-pattern and horizontal slits for a stable grasp under both dry and oily conditions. To determine the structure, we reinvestigated the fingertip deformation in the experiment shown in Fig. 4. In this case, we focused on the side view (Fig. 19) and investigated how the interval of the horizontal slits changed with the loading under the oily condition. Following loading, the slits around the upper area expanded, while the slits around the lower area compressed. This change in size increased the area of the oil stands and R in (1) (given in the Appendix), and provided the increase in fluid film thickness leading to the decrease in friction at the upper area. The lower area improved at gripping because of antipodal reasons. Therefore, the slits around the upper area did not perform well.

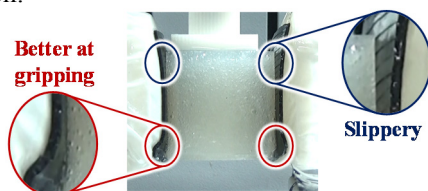


Fig. 19. Side view of the object grasped by the fingertip with the horizontal slit texture patterns after applying a load under the oily condition; investigation of how the slit interval changed with loading

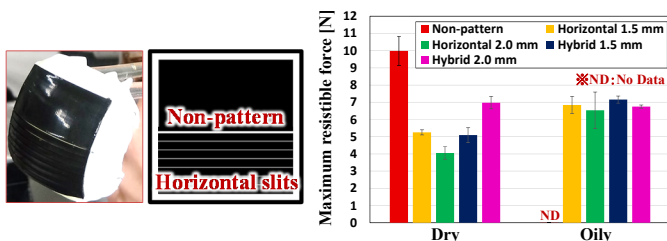


Fig. 20. Fluid fingertip with a hybrid texture pattern of non-pattern and horizontal slits

Fig. 21. Maximum resistible force for the hybrid texture pattern considering a single loading direction

A. Considering a single loading direction

Based on this, we propose the new slit texture pattern shown in Fig. 20 for a stable grasp under both dry and oily conditions. It is a hybrid structure of the non-pattern in the upper area and horizontal slit pattern in the lower area.

The effectiveness of the proposed hybrid texture pattern was investigated by the same experiment shown in Fig. 4. Considering the effect of the slit interval, we investigated the cases when the slit interval was 1.5 and 2.0 mm, which demonstrated the best and second-best performances, respectively. For comparison, the non-pattern and horizontal slits were also investigated. Fig. 21 shows the results where the hybrid texture with the slit interval of 2.0 mm showed the higher performance of both the conditions. Under the oily condition, similar performances were achieved with the

exception of the non-pattern. Under the dry condition, the hybrid texture with a slit interval of 2.0 mm exhibited an intermediate performance between the non-pattern and horizontal slits. In contrast, at the interval of 1.5 mm, the performance was nearly half of the one at the non-pattern texture. The non-pattern area for the hybrid texture is half of all the area, and the contribution of the non-pattern area on the performance was considered close to half of the performance for the non-pattern texture. It is then considered that at the interval of 1.5 mm, the slit part did not perform well for an increase in resistible force, because of the low rigidity/stiffness in the bending resulting from the small interval, indicated by the analysis of the results in Fig. 18. The stress at the lower part was larger than that at the upper part [50], and, therefore, the slit area with a relatively large interval was required for a good performance in the hybrid texture.

B. Concentric hybrid texture pattern

The hybrid texture shown in Fig. 20 can only accommodate a single loading direction. For real tasks, the grasping posture can be changed by a robotic arm, and then the loads in arbitrary directions should be considered. Here, we proposed the concentric hybrid texture pattern displayed in Fig. 22 so that the pattern could be a local hybrid non-pattern and horizontal pattern in any arbitrary direction on the contact surface. It is a hybrid structure of the non-pattern in the center area and circular slits in the outer area.

The following fabrication procedure was used. First, a flat surface made of silicone sealant was molded on a polypropylene sheet. Next, the surface was slit by a compass cutter. Following this, a rubber film (fingertip surface) was bonded to the slit surface. After solidification, the sheet was removed and the surface texture was obtained.

The effectiveness of the new texture was examined. The diameter of the texture area was 35 mm, and the diameter of the non-pattern area was set to 15 mm such that the contact area includes the outer concentric slits while grasping the target object (the silicone cube). Let ΔR be the slit interval for the outer concentric slits. We investigated the performances for various ΔR (1.0, 1.5, 2.0, 2.5, 3.0 mm). Fig. 23 shows the results where the non-pattern texture was fabricated by the same method as the concentric hybrid texture pattern. The maximum resistible force increased with the slit interval under the dry condition, while the force decreased under the oily condition. At the interval of 1.0 mm, the performance under the oily condition was better than that under the dry condition. The result indicates that the concentric texture performed well. At the interval of 1.5 mm, the performance was inverted; the performance under the oily condition was lower than that under the dry condition. A similar trend was observed with the results for the intervals of 1.5 and 2.0 mm in the case of the liner hybrid pattern, as exhibited in Fig. 21. The results indicate that a change in arrangement to the concentric texture caused it to perform well (an increase in resistible force) in all directions, although the required slit interval for good performance was different. It should be noted that the fabrication process of pressing the textures produced smoother surfaces, which led to

increases in friction and rigidity/stiffness in bending. The different values were then observed with the results in Figs. 21 and 23, especially under the dry condition.

C. Grasping test

To see the effectiveness of the concentric hybrid texture in actual object grasping, a grasping test was conducted. The target objects presented in Fig. 24 were selected. Considering the actual situations, the target objects could be handled under wet or oily conditions. It should be noted that silken tofu was normally graspable by conventional fluid fingertips [20]–[23], but after leaving the tofu on a table for a few hours, the water exuded and the friction decreased. Then, the conventional fluid fingertips failed to grasp the tofu under the wet condition. Here, we investigated the grasping under the wet condition. The other target objects were investigated under dry and oily conditions. We also investigated various slit intervals of 1.0–3.0 mm. Table 1 summarizes the success rate of the grasping. The objects were grasped successfully under the dry conditions. The small intervals of 1.0 and 1.5 mm performed well under both conditions. The other intervals showed the performance associated with the results shown in Fig. 23. The results confirmed the validity of the concentric hybrid texture pattern.

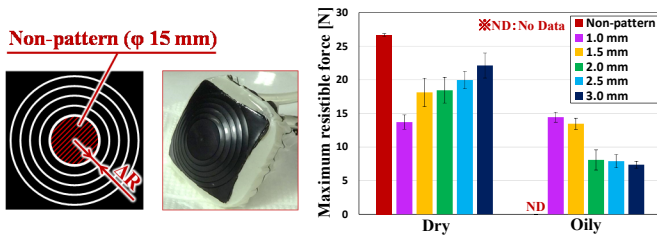


Fig. 22. Concentric hybrid texture pattern

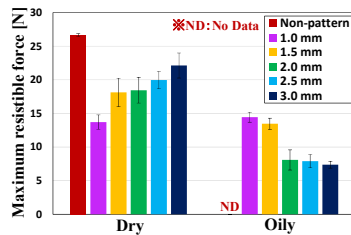


Fig. 23. Maximum resistible force for the concentric hybrid texture pattern



Fig. 24. Target objects for grasping test

TABLE I
SUCCESS RATE OF GRASPING

Object	Size	Condition	1.0 mm	1.5 mm	2.0 mm	2.5 mm	3.0 mm
Silken Tofu	35 ³ mm ³ 35 g	Wet	4/4	4/4	3/4	3/4	1/4
		Dry	4/4	4/4	4/4	4/4	4/4
Bearing	Φ35 mm 40 g	Dry	4/4	4/4	4/4	4/4	4/4
		Oily	4/4	4/4	4/4	3/4	3/4
Ramekin	Φ52 mm 43 g	Dry	4/4	4/4	4/4	4/4	4/4
		Oily	4/4	4/4	4/4	4/4	3/4

VI. CONCLUSION

In this study, we investigated the effect of surface texture patterns on the maximum resistible force with the aim of stable grasping under both wet and dry conditions. We proposed hybrid texture patterns with stable grasping under both conditions. The maximum resistible force is the maximum tangential force at which the fingertip can maintain contact when applying and increasing the tangential/shear force, which

was postulated in some previous studies [25] [26]. This is related to the friction and fingertip deformation. Stable grasp was defined as the capability of balancing large external forces or moments during grasping. The texture patterns were evaluated by the maximum resistible force. To attain a large contact area that facilitates a large resistible force, as suggested by the preliminary experimental results, we considered slit texture patterns. Under the dry condition, the non-pattern performed the best, whereas under the wet (oily) condition, the horizontal slit pattern performed the best. Additionally, for the horizontal slit pattern, the maximum resistible force under the oily condition was larger than that under the dry condition. A slit interval of 1.5 mm and fluid pressure of 2 kPa showed the best performance. Based on these results, the concentric hybrid texture pattern was proposed for stable grasping under the dry and wet conditions. The grasping test showed the effectiveness of the proposed pattern. Note that only the primary patterns were investigated in this study. The optimization of the surface pattern including the investigation of irregular intervals and shapes under various conditions and the investigations for the other types of fingertips will be studied in the future.

APPENDIX: ELASTOHYDRODYNAMIC LUBRICATION

A fluid film at the contact area can provide lubrication. If the contact area is elastically deformable, the lubrication becomes an elastohydrodynamic lubrication (EHL) [49], [50]. As the targeted surface patterns were elastic, we introduced EHL theory. Each segment of the patterns had a width with respect to the sliding direction of the fluid, then, the Ertel–Grubin model [50], [51] was adopted assuming line contact (contact between a flat surface and cylinder):

$$h_0 = 1.95(\alpha\eta_0 u)^{8/11}(EL)^{1/11}W^{-1/11}R^{4/11} \quad (1)$$

where h_0 is the film thickness, α and η_0 are the parameters of the Barus equation modeling the relationship between viscosity and pressure, u is the sliding velocity, E is the equivalent Young's modulus for two materials constructing the contact, L is the width of the contact area, W is the load (grasping force), and R is the equivalent contact radius. The equation was derived by combining the Reynolds equation representing hydrodynamics, Barus equation, and Hertz theory representing the contact between elastic bodies. It should be noted that from Newton's law of viscosity, friction increases with the decrease in h_0 .

REFERENCES

- [1] "Technology that supports dish washing with kitchen robots," 2008.
- [2] K. C. Galloway, K. P. Becker, B. Phillips, J. Kirby, S. Licht, D. Tchernov, R. J. Wood, and D. F. Gruber, "Soft Robotic Grippers for Biological Sampling on Deep Reefs," *Soft Robot.*, vol. 3, no. 1, pp. 23–33, Mar. 2016.
- [3] H. S. Stuart, S. Wang, B. Gardineer, D. L. Christensen, D. M. Aukes, and M. Cutkosky, "A compliant underactuated hand with suction flow for underwater mobile manipulation," *Proc. of IEEE Int. Conf. Robot. Autom.*, pp. 6691–6697, 2014.
- [4] K. B. Shimoga and A. A. Goldenberg, "Soft Robotic Fingertips: Part I: A Comparison of Construction Materials," *Int. J. Rob. Res.*, vol. 15, no. 4, pp. 320–334, Aug. 1996.

- [5] M. Tavakoli and A. T. de Almeida, "Adaptive under-actuated anthropomorphic hand: ISR-SoftHand," in *2014 IEEE/RSJ Int. Conf. on Intelligent Robots and Systems*, 2014, pp. 1629–1634.
- [6] M. Tavakoli, R. Batista, and L. Sgrigna, "The UC SoftHand: Light Weight Adaptive Bionic Hand with a Compact Twisted String Actuation System," *Actuators*, vol. 5, no. 1, p. 1, Dec. 2015.
- [7] H. Takeuchi and T. Watanabe, "Development of a multi-fingered robot hand with softness-changeable skin mechanism," in *Joint 41st Int. Symposium on Robotics and 6th German Conf. on Robotics 2010, ISR/ROBOTIK 2010*, 2010, vol. 1, pp. 606–612.
- [8] A. Pettersson, S. Davis, J. O. O. Gray, T. J. J. Dodd, and T. Ohlsson, "Design of a magnetorheological robot gripper for handling of delicate food products with varying shapes," *J. Food Eng.*, vol. 98, no. 3, pp. 332–338, 2010.
- [9] R. Deimel and O. Brock, "A compliant hand based on a novel pneumatic actuator," in *2013 IEEE Int. Conf. on Robotics and Automation*, 2013, pp. 2047–2053.
- [10] R. Deimel and O. Brock, "A novel type of compliant and underactuated robotic hand for dexterous grasping," *Int. J. Rob. Res.*, vol. 35, no. 1–3, pp. 161–185, Jan. 2016.
- [11] F. Ilievski, A. D. Mazzeo, R. F. Shepherd, X. Chen, and G. M. Whitesides, "Soft Robotics for Chemists," *Angew. Chemie Int. Ed.*, vol. 50, no. 8, pp. 1890–1895, Feb. 2011.
- [12] A. Dameitry and H. Tsukagoshi, "Lightweight Underactuated Pneumatic Fingers Capable of Grasping Various Objects," in *IEEE Int. Conf. on Robotics and Automation*, 2016, pp. 2009–2014.
- [13] A. a Stokes, R. F. Shepherd, S. a Morin, F. Ilievski, and G. M. Whitesides, "A Hybrid Combining Hard and Soft Robots," *Soft Robot.*, vol. 1, no. 1, pp. 70–74, Mar. 2014.
- [14] J. Kim, A. Alspach, and K. Yamane, "3D printed soft skin for safe human-robot interaction," in *2015 IEEE/RSJ Int. Conf. on Intelligent Robots and Systems (IROS)*, 2015, pp. 2419–2425.
- [15] H. Choi, M. Koc, and M. Koç, "Design and feasibility tests of a flexible gripper based on inflatable rubber pockets," *Int. J. Mach. Tools Manuf.*, vol. 46, no. 12–13, pp. 1350–1361, 2006.
- [16] R. F. Shepherd, A. A. Stokes, R. M. D. Nunes, and G. M. Whitesides, "Soft Machines That are Resistant to Puncture and That Self Seal," *Adv. Mater.*, vol. 25, no. 46, pp. 6709–6713, Dec. 2013.
- [17] B. S. Homborg, R. K. Katschmann, M. R. Dogar, and D. Rus, "Haptic identification of objects using a modular soft robotic gripper," in *2015 IEEE/RSJ Int. Conf. on Intelligent Robots and Systems (IROS)*, 2015, pp. 1698–1705.
- [18] E. Brown, N. Rodenberg, J. Amend, A. Mozeika, E. Steltz, M. R. Zakin, H. Lipson, and H. M. Jaeger, "Universal robotic gripper based on the jamming of granular material," *Proc. Natl. Acad. Sci.*, vol. 107, no. 44, pp. 18809–18814, Nov. 2010.
- [19] J. R. Amend, E. Brown, N. Rodenberg, H. M. Jaeger, and H. Lipson, "A Positive Pressure Universal Gripper Based on the Jamming of Granular Material," *IEEE Trans. Robot.*, vol. 28, no. 2, pp. 341–350, Apr. 2012.
- [20] R. Maruyama, T. Watanabe, and M. Uchida, "Delicate grasping by robotic gripper with incompressible fluid-based deformable fingertips," in *2013 IEEE/RSJ Int. Conf. on Intelligent Robots and Systems*, 2013, pp. 5469–5474.
- [21] R. Adachi, Y. Fujihira, and T. Watanabe, "Identification of danger state for grasping delicate tofu with fingertips containing viscoelastic fluid," *IEEE/RSJ Int. Conf. Intell. Robot. Syst.*, pp. 497–503, 2015.
- [22] T. Nishimura, Y. Fujihira, R. Adachi, and T. Watanabe, "New Condition for Tofu Stable Grasping with Fluid Fingertips," *Proc. IEEE Int. Conf. Autom. Sci. Eng.*, 2016.
- [23] T. Nishimura, Y. Fujihira, and T. Watanabe, "Microgripper-embedded fluid fingertipenhancing positioning and holding abilities for universal grasping," *J. Mech. Robot.*
- [24] T. Nishimura, K. Mizushima, Y. Suzuki, T. Tsuji, and T. Watanabe, "Variable-Grasping-Mode Underactuated Soft Gripper With Environmental Contact-Based Operation," *IEEE Robot. Autom. Lett.*, vol. 2, no. 2, pp. 1164–1171, Apr. 2017.
- [25] T. Watanabe and Y. Fujihira, "Experimental investigation of effect of fingertip stiffness on friction while grasping an object," in *2014 IEEE Int. Conf. on Robotics and Automation (ICRA)*, 2014, pp. 889–894.
- [26] Y. Fujihira, K. Harada, T. Tsuji, and T. Watanabe, "Experimental investigation of effect of fingertip stiffness on resistible force in grasping," in *2015 IEEE Int. Conf. on Robotics and Automation (ICRA)*, 2015, pp. 4334–4340.
- [27] P. Tiezzi, I. Kao, and G. Vassura, "Effect of layer compliance on frictional behavior of soft robotic fingers," *Adv. Robot.*, vol. 21, no. 14, pp. 1653–1670, Jan. 2007.
- [28] P. Tiezzi and I. Kao, "Modeling of Viscoelastic Contacts and Evolution of Limit Surface for Robotic Contact Interface," *IEEE Trans. Robot.*, vol. 23, no. 2, pp. 206–217, 2007.
- [29] N. Xydias, "Modeling of Contact Mechanics and Friction Limit Surfaces for Soft Fingers in Robotics, with Experimental Results," *Int. J. Rob. Res.*, vol. 18, no. 9, pp. 941–950, 1999.
- [30] I. Kao and F. Yang, "Stiffness and contact mechanics for soft fingers in grasping and manipulation," *Robot. Autom. IEEE Trans.*, vol. 20, no. 1, pp. 132–135, 2004.
- [31] I. Kao and M. R. Cutkosky, "Quasistatic Manipulation with Compliance and Sliding," *Int. J. Rob. Res.*, vol. 11, no. 1, pp. 20–39, 1992.
- [32] T. Inoue and S. Hirai, "Elastic Model of Deformable Fingertip for Soft-Fingered Manipulation," *IEEE Trans. Robot.*, vol. 22, no. 6, pp. 1273–2379, 2006.
- [33] V. Anh Ho and S. Hirai, "Modeling and Analysis of a Frictional Sliding Soft Fingertip, and Experimental Validations," *Adv. Robot.*, vol. 25, no. 3–4, pp. 291–311, Jan. 2011.
- [34] M. Ciocarlie, C. Lackner, and P. Allen, "Soft Finger Model with Adaptive Contact Geometry for Grasping and Manipulation Tasks," in *Second Joint EuroHaptics Conf. and Symposium on Haptic Interfaces for Virtual Environment and Teleoperator Systems (WHC'07)*, 2007, pp. 219–224.
- [35] T. Watanabe, "Softness effects on manipulability and grasp stability," in *2011 IEEE/RSJ Int. Conf. on Intelligent Robots and Systems*, 2011, pp. 1398–1404.
- [36] "Moley — The world's first robotic kitchen."
- [37] R. B. Rusu, B. Gerkey, and M. Beetz, "Robots in the kitchen: Exploiting ubiquitous sensing and actuation," *Rob. Auton. Syst.*, vol. 56, no. 10, pp. 844–856, 2008.
- [38] K. Okada, M. Kojima, S. Tokutsu, Y. Mori, T. Maki, and M. Inaba, "Task guided attention control and visual verification in tea serving by the daily assistive humanoid HRP2JSK," *2008 IEEE/RSJ Int. Conf. Intell. Robot. Syst. IROS*, pp. 1551–1557, 2008.
- [39] K. Okada, M. Kojima, Y. Sagawa, T. Ichino, K. Sato, and M. Inaba, "Vision based behavior verification system of humanoid robot for daily environment tasks," *Proc. 2006 6th IEEE-RAS Int. Conf. Humanoid Robot. HUMANOIDS*, pp. 7–12, 2006.
- [40] M. Dadkhah, Z. Zhao, N. Wettels, and M. Spenko, "A Self-Aligning Gripper Using an Electrostatic / Gecko-Like Adhesive," *2016 IEEE/RSJ Int. Conf. Intell. Robot. Syst.*, 2016.
- [41] E. W. Hawkes, D. L. Christensen, Amy Kyungwon Han, H. Jiang, and M. R. Cutkosky, "Grasping without squeezing: Shear adhesion gripper with fibrillar thin film," in *2015 IEEE Int. Conf. on Robotics and Automation (ICRA)*, 2015, vol. 2015–June, no. June, pp. 2305–2312.
- [42] A. Tsipenyuk and M. Varenberg, "Use of biomimetic hexagonal surface texture in friction against lubricated skin.," *J. R. Soc. Interface*, vol. 11, no. 94, p. 20140113, 2014.
- [43] M. Varenberg and S. N. Gorb, "Hexagonal surface micropattern for dry and wet friction," *Adv. Mater.*, vol. 21, no. 4, pp. 483–486, 2009.
- [44] D. M. Drotleff, L. Stepien, M. Kappl, W. J. P. Barnes, H. J. Butt, and A. Del Campo, "Insights into the adhesive mechanisms of tree frogs using artificial mimics," *Adv. Funct. Mater.*, vol. 23, no. 9, pp. 1137–1146, 2013.
- [45] T. YAMAGUCHI and K. HOKKIRIGAWA, "Development of a High Slip-resistant Footwear Outsole Using a Hybrid Rubber Surface Pattern," *Ind. Health*, vol. 52, no. 5, pp. 414–423, 2014.
- [46] T. Yamaguchi, J. Hsu, Y. Li, and B. E. Maki, "Efficacy of a rubber outsole with a hybrid surface pattern for preventing slips on icy surfaces," *Appl. Ergon.*, vol. 51, pp. 9–17, Nov. 2015.
- [47] S. SASAKI, "Surface Texturing for Improvement of Tribological Properties," *J. Surf. Finish. Soc. Japan*, vol. 65, no. 12, pp. 568–572, 2014.
- [48] K. Matsuda, D. Hashimoto, and K. Nakamura, "Real contact area and friction property of rubber with two-dimensional regular wavy surface," *Tribol. Int.*, vol. 93, pp. 523–529, Jan. 2016.
- [49] D. Dowson, G. R. Higginson, J. F. Archard, and A. W. Crook, *Elasto-hydrodynamic lubrication*. Pergamon Press, 1977.
- [50] J. Williams, *Engineering Tribology*. Cambridge: Cambridge University Press, 2005.
- [51] A. Grubin, I. Vinogradova, and K. Ketova, "Investigation of the contact of machine components," 1949.